Influence of Motion Restrictions in an Ankle Exoskeleton on Force Myography in Straight and Curve Walking

Charlotte Marquardt, Miha Dežman, and Tamim Asfour

***Abstract*— Exoskeletons impose kinematic constraints on the user's motion and thus impact their muscle activity. In this paper, we assess the impact of mechanical simplifications on the functionality and efficiency of force myography (FMG)-based muscle activity sensor systems in an un-powered ankle exoskeleton. For this purpose, the FMG signals of the *gastrocnemius medialis*, *gastrocnemius lateralis*, and *tibialis anterior* muscles of six healthy participants were recorded without and with an ankle exoskeleton during straight and curve walking. Three different DoF configurations of the exoskeleton were analyzed. The results show notable changes when both in-/eversion and internal/external rotation were restricted compared to walking without an exoskeleton. However, due to consistent movement in the soft tissue, an exclusive locking of internal/external rotation does not lead to notable effects. The most substantial changes in the FMG signal during curve walking were observed in the *gastrocnemius lateralis* muscle. Leg and curve-dependent changes in the FMG signal were identified, which are similar to changes in the EMG signal and adaptations of gait mechanics reported in previous studies.**

I. Introduction

Over the years, a variety of assistive exoskeletons have been developed for the assistance of the ankle joint [1], [2]. The ankle joint, being the primary contributor to human locomotion, plays a crucial role in walking. However, despite numerous attempts to design compact and lightweight systems, the availability of portable and untethered ankle mechanisms that adequately meet anatomical requirements and support natural movement is limited [2].

The ankle joint possesses three degrees of freedom (DoF), namely plantar-/dorsiflexion (PF/DF), in-/eversion (IN/EV), and internal/external rotation (IR/ER). These combined motions facilitate pronation and supination of the foot during walking. Although exoskeletons that assist the ankle joint solely in the sagittal plane have shown benefits in reducing metabolic costs [3], these devices need to replicate human-like functions without impeding the user's movement to effectively preserve human balance [4]. Studies indicate that while IN/EV and IR/ER are less prominent, they still contribute to walking both on straight and curved paths [2], [5]. However, assisting while allowing motion on the three DoF of the ankle increases the mechanical complexity of the exoskeleton and adds weight, which might diminish the benefits of assistance [6].

This work has been supported by the Carl Zeiss Foundation through the JuBot project.

The authors are with the High Performance Humanoid Technologies Lab, Institute for Anthropomatics and Robotics, Karlsruhe Institute of Technology (KIT), Germany. {charlotte.marquardt, asfour}@kit.edu

The use of knowledge from joint biomechanics and kinematics can result in substantial advancements in the development of exoskeleton mechanisms and their control. While joint kinematics and kinetics are well-established factors in the design and control of exoskeletons, integrating direct biofeedback from the musculoskeletal system has the potential to enhance exoskeleton control design [7].

Measurement of muscle activation and interaction forces between the user and the exoskeleton provides valuable data and insights into both the recognition of human motion intention and the specific joints involved in motion. This improves the robustness of the control of prosthetics, orthotics, and exoskeletons [8]. The activation of human muscles involves the electrical stimulation of muscle fibers, which subsequently triggers a mechanical response in the form of fiber contraction. This results in alterations in muscle stiffness and shape. Electromyography (EMG) stands as a widely recognized approach for detecting electrical muscle activity [9]–[11]. EMG signal quality is affected by skin-electrode contact, electrode slippage, skin changes like sweating, extensive post-processing, and electrical noise vulnerability.

In contrast, FMG detects the mechanical phenomena associated with muscle contraction, rather than electrical effects, and therefore is not dependent on contact with the bare skin and is not affected by electrical noise. The use of FMG has been extensively and successfully investigated in various wearable applications such as upper arm or hand motion classification and intention detection [12]–[14], lower limb gait phase or event detection, ankle po-

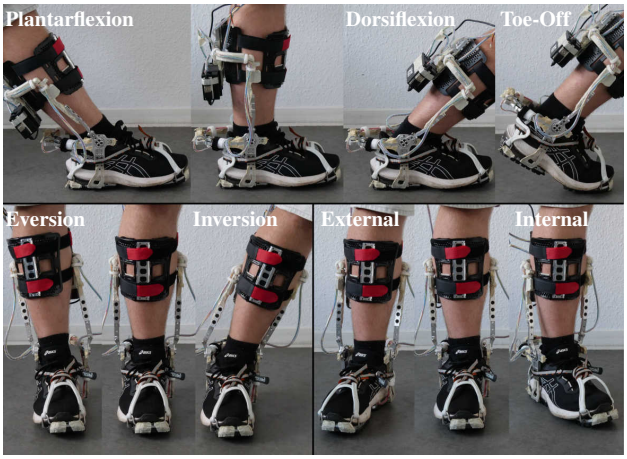

Fig. 1: Ankle exoskeleton allowing all three biological DoF (adapted from [2]).

sition classification [15]–[17], step counting [18] or joint position/angle estimation [19], [20]. The requirements and manner of attachment of FMG sensors differs compared to the EMG electrodes. Whereas EMG electrodes are attached or glued to the skin to enable good electrical conductivity. Contrary to that, the FMG sensors require a constant normal force pushing them onto the body to ensure the quality of the signals. This demonstrates that FMG technology is a promising alternative to EMG technology to create more versatile exoskeleton devices. In our previous work [21], we introduced a compact, low-profile barometer-based FMG sensor unit. The sensor unit robustly measures the normal forces resulting from changes in surface muscle pressure and is now integrated into the cuffs of the ankle exoskeleton presented in [2].

The descriptive quality of FMG signals changes depending on the motion task. When walking on a curved path, the center of mass (CoM) is shifted toward the inner foot causing a redistribution of load on both feet. This redistribution of force alters the muscular action patterns, as previously recognized in EMG signals [22]–[25], and is expected to produce a similar effect in FMG signals. The mechanical effect of muscle activity is also influenced by the constraints an exoskeleton imposes on the user's motion. The effects of constraining motions of an un-powered ankle joint exoskeleton on EMG have been reported in [26]. In their study with one subject, muscle activation was measured using EMG in the six primary lower limb muscles used during straight walking. The root-mean-square features indicated significant changes in muscle activity using an exoskeleton constraining non-sagittal motion. Hence, it is crucial to assess the biomechanical effects that arise from various design simplifications made in the design of the ankle exoskeleton mechanism. Wearing an exoskeleton device that restricts ankle motion to one degree of freedom (DoF) could produce different signals of FMG compared to a less restrictive exoskeleton with three DoF. Evaluating the FMG technology in various exoskeletons would provide more insight into the robustness of this technology for wider use. To date, it has not yet been investigated how kinematic obstructions introduced by an exoskeleton influence FMG signals.

The contribution of this paper is an assessment of the influence of reduced DoF in an ankle exoskeleton on the FMG signal in the muscles of the lower limb during straight and curve-walking. The findings will contribute to clarifying the impact of mechanical simplifications on the functionality and efficiency of FMG-based muscle activity sensor systems in ankle exoskeletons. This can guide future improvements in the design and control of such exoskeletons.

The rest of the paper is organized as follows. Section II describes the ankle exoskeleton design and Section III describes the user study carried out. The methods used to analyze the collected data are given in Section IV. The results are presented in Section V and discussed in Section VI. Section VII concludes the paper.

II. Exoskeleton Design and Sensor Setup

The ankle exoskeleton utilized in this paper is described in [2]. It consists of a foot and a shank frame and weighs 1.8 kg. The foot frame is manually adaptable in size to different shoe sizes. It allows rolling over from the heel to the toes during motion. The shank frame includes a parallelogram mechanism allowing for all three human DoF of the ankle joint as shown in Figs. 1 and 2a. The design includes two independent hinge joints (orange), one on each side of the frame, to allow PF/DF. In combination with two additional orthogonal hinge joints just above the latter hinge joints (blue), one on each side, and a central hinge joint at the calf of the user (orange) it provides IN/EV. An additional set of ball joints at the top of the side rods (blue), one on each side, enables IR/ER. In all experiments presented in this paper, the exoskeleton is used passively; however, its design allows for future cable-driven actuation of plantar flexion.

Different exoskeleton DoF have to be blocked to simulate a one, two, or three DoF exoskeleton and therefore influence the level of constraints imposed on the user. Figure 2 shows how DoF reduction is achieved in the three exoskeleton configurations. The configuration *Exo2DoF* (Fig. 2b) is achieved by adding a bent frame (red) connecting both side rods, restricting the hinge joints on both sides to move independently and thus block IR/ER. Blocking the two hinge joints at the side together with the calf hinge joint blocks IN/EV and leads to the *Exo1DoF* configuration (Fig. 2c).

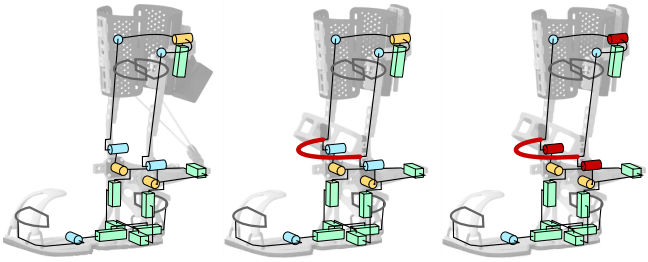

(a) *Exo3DoF* (b) *Exo2DoF* (c) *Exo1DoF*

Fig. 2: Ankle exoskeleton motion restriction. The kinematic structure consists of "" hinge joints, "" ball joints, "" hinge joints with encoder, "" adjustable translation joints and "" blocked hinge joints (adapted from [2]).

The FMG sensor unit previously described in [21] measures the normal force resulting from a change in volume and stiffness of the human muscle underneath the cuff during leg motion. The sensor unit consists of five barometric pressure sensors on one single printed circuit board (PCB) covered by a silicon dome as shown in Fig. 3.

Three FMG sensor units were integrated into the shank cuffs of the ankle exoskeleton (Fig. 3). The units are positioned on anatomically relevant locations to measure the activity of *gastrocnemius medialis (GM)*, *gastrocnemius lateralis (GL)* and *tibialis anterior (TA)*. The placement also complies with the findings from [21] regarding sensor-muscle misalignment.

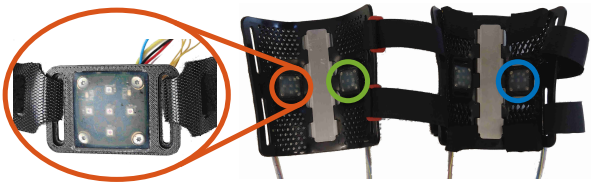

Fig. 3: Three FMG sensor units integrated in the exoskeleton cuffs at the positions of the extensor and flexor muscles *GM* (green), *GL* (orange) and *TA* (blue).

III. User Study

To study the effect of restricting the motion of an ankle exoskeleton on FMG, a user study was conducted in a controlled laboratory setting. The experiment protocol was approved by the Karlsruhe Institute of Technology (KIT) Ethics Committee under the ethical approval of the JuBot project.

Six healthy participants (m = 4, f = 2) participated in the study. All participants provided their informed consent in writing before the experiment and all procedures were performed in accordance with the Declaration of Helsinki. The participant information is given in Table I.

TABLE I: Participant Information

Height [cm]	Weight [kg]	EU shoe size	Age [y]
177.7 ± 9.3	77.7 ± 24.9	42.7 ± 2.5	24.5 ± 2.6

Values represent the mean and standard deviation.

In the user study, a complete experiment was conducted once without an exoskeleton to provide a baseline for the analysis. During the use of the exoskeleton, the PF/DF remained unrestricted throughout the whole experiment. The four experimental configurations (Fig. 4) were defined, according to the most often occurring DoF combinations in ankle exoskeletons [27], as follows

1) *NoExo*: participants perform the tasks without the exoskeleton,
2) *Exo3DoF*: participants wear the exoskeleton with all three ankle DoF available,
3) *Exo2DoF*: the internal and external rotation of the ankle is restricted,
4) *Exo1DoF*: the exoskeleton is reduced to allow only PF/DF.

The three exoskeleton configurations were applied in a randomized order.

In each configuration, the participants performed the following two tasks at a self-selected speed. Each task was repeated four times and initialized by standing upright on both feet where calibration data was recorded.

- *Walk straight*: In this task, users walk along a straight 3 m long path. In the end, they turn around 180° and walk to the start position, where they again turn around 180° and return to their starting pose.
- Walk eight: Users walk in an eight-shaped path with a diameter of each circle of about 1.5 m (marked with tape), starting in the middle of the eight and stopping once they are at the starting position again. There are two variants for this task, i. e. starting with turning left and turning right. The task was later segmented into *walk left* and *walk right* depending on the curve direction.

The ankle exoskeleton was adjusted prior to the experiment to fit each participant and ensure the best alignment of the joint axes. Furthermore, participants received a second foot frame (0.65 kg) on their left foot to mitigate the impact of different leg lengths. After each change of configuration, the participants were allowed to familiarize themselves with the exoskeleton in a self-chosen interval of not more than 3 min. In the *NoExo* configuration, participants were equipped with the shank cuff of the exoskeleton whose height was marked on the user's leg with the use of the exoskeleton to provide comparable measurements of the FMG signal.

To ensure consistency throughout the experiments, all participants wore the same type of sports shoes provided by the authors. The shoes included a force sensing resistor (FSR) sensor placed below the heel to detect contact with the ground. The pressure resulting from muscular activity was recorded through the aforementioned FMG sensor units, and the angles of the human and exoskeleton joints were recorded through integrated absolute encoders and motion capture (Fig. 5 A). Video recordings of the experiments were available. The analysis of the results has been deliberately focused on the FMG signal, and the evaluation of the effects on the kinematic parameters can be found in [28].

IV. Data Analysis

Post-processing of the experimental data included calibration based on the data collected during the initial standing before each task. Segmentation of relevant data for each task and configuration according to the gait cycle was performed based on the heel strike, detected by a FSR sensor placed underneath the heel inside the participant's shoe (Fig. 5 B) and validated based on the video recordings. All transient strides have been removed. All tasks were segmented so that only full gait cycles in each direction were considered. Walk eight was segmented into two separate directions (Fig. 5 C), turning left and right, respectively, where the considered leg

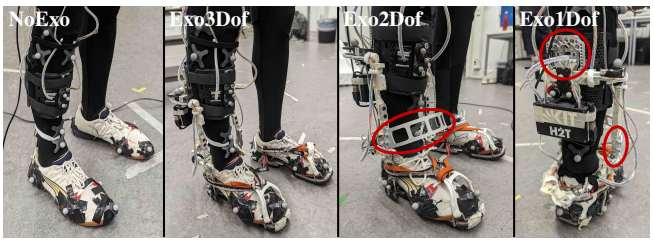

Fig. 4: Participant without and with the ankle exoskeleton in the four experimental configurations. The parts added to block certain DoF are marked in red.

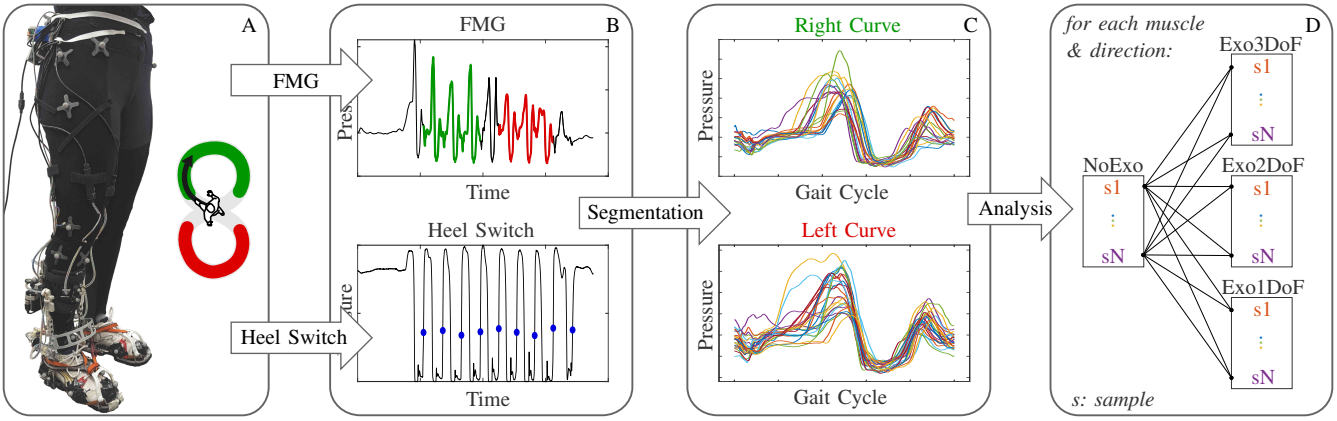

Fig. 5: Overview of the data acquisition (A), post-processing (B), segmentation (C) into directions and analysis (D) per sample *sN* shown exemplary for the data of the task walk eight and the comparison of configurations in one participant. A sample is equivalent to one complete gait cycle of the respective experiment.

corresponds to the outer leg in a left curve and to the inner leg in a right curve. For the FMG sensor unit, the mean signal of the five barometric sensors was calculated within one unit. The resulting data was normalized per participant according to their measured absolute maximum and minimum values per muscle to compare the data of all participants with each other.

Data was analyzed in two aspects: 1) the differences identified between various configurations within a single direction to assess the impact of DoF reduction, and 2) the influence of curve walking on muscle activity compared to straight walking expecting a greater effect of ankle motion restriction due to a larger range of motion (RoM) of IN/EV and IR/ER [2].

The FMG signal error of the three exoskeleton configurations relative to the motion without the exoskeleton was calculated as the difference between those signals. Each sample of each configuration was compared to each single sample of the *NoExo* condition (Fig. 5 D). A sample is equivalent to one complete gait cycle of the respective experiment. A comparison of the curve walking in both directions with *walk straight* as a baseline was conducted similarly. A positive error corresponds to the FMG magnitude being higher than the baseline signal and vice versa. The closer the error is to zero, the more similar the signal is, and thus the more natural the trajectory of the signal is. Both the mean error and its standard deviation were determined.

To compare the occurrence of the peak muscle activity (FMG) throughout the gait cycle, the peak amplitude of each sample and its respective time stamp (in percent of the gait cycle) was calculated. Both the mean and its standard deviation were then determined.

V. Results

This section presents the results of our user study with a focus on both the various configurations and walking directions. Figures 6 and 7 show the characteristics of the FMG signal while walking along the three locomotor paths in the four different configurations. Table II presents the mean occurrence of the peak amplitude of the FMG signal within the gait cycle.

The top three plots in Fig. 6 show the behavior of the mean muscle pressures throughout the gait cycle and in all four configurations (*NoExo*, *Exo3DoF*, *Exo2DoF*, *Exo1DoF*) in the direction *walk straight* (as average of all participants). The trajectory of the mean pressure for all three exoskeleton configurations shows more prominent peaks in the GM just before the toe lift (about 47 % of the gait cycle) and in the TA at the beginning of the stance phase (about 18 % of the gait cycle) compared to walking without an exoskeleton. The GL displays a wider activation with a less noticeable peak just before toe lift (about 44 % of the gait cycle). However, TA does not show any noticeable peak in the *NoExo* configuration, but rather a constant activation of the muscle during the complete stance phase.

The diagram in the bottom of Fig. 6 shows a comparison between the FMG signal of each configuration (*Exo3DoF*, *Exo2DoF*, *Exo1DoF*) with the *NoExo* configuration for each muscle (GM, GL, TA) and direction (*walk straight*, *walk left*, *walk right*). The mean values for each muscle are represented by black horizontal lines, while the colored bars represent the standard deviation. In most directions and muscles, the *Exo1DoF* configuration has the highest mean error of the *NoExo* configuration, apart from the TA muscle, when walking right. The *Exo2DoF* and *Exo3DoF* configurations show more similarity between tasks, with the *Exo2DoF* configuration featuring smaller errors in the TA muscle across all three tasks.

Figure 7 shows the mean FMG signal (average of the mean behavior of the curve of all participants) of the three muscles (GM, GL, TA) over the normalized time interval of the gait cycle when walking in all three directions (*walk straight*, *walk left*, *walk right*) for all four configurations (*NoExo*, *Exo3DoF*, *Exo2DoF*, *Exo1DoF*). The signals of the different walking directions are aligned at the time of the heel strike and identified by dashed and dotted lines, respectively.

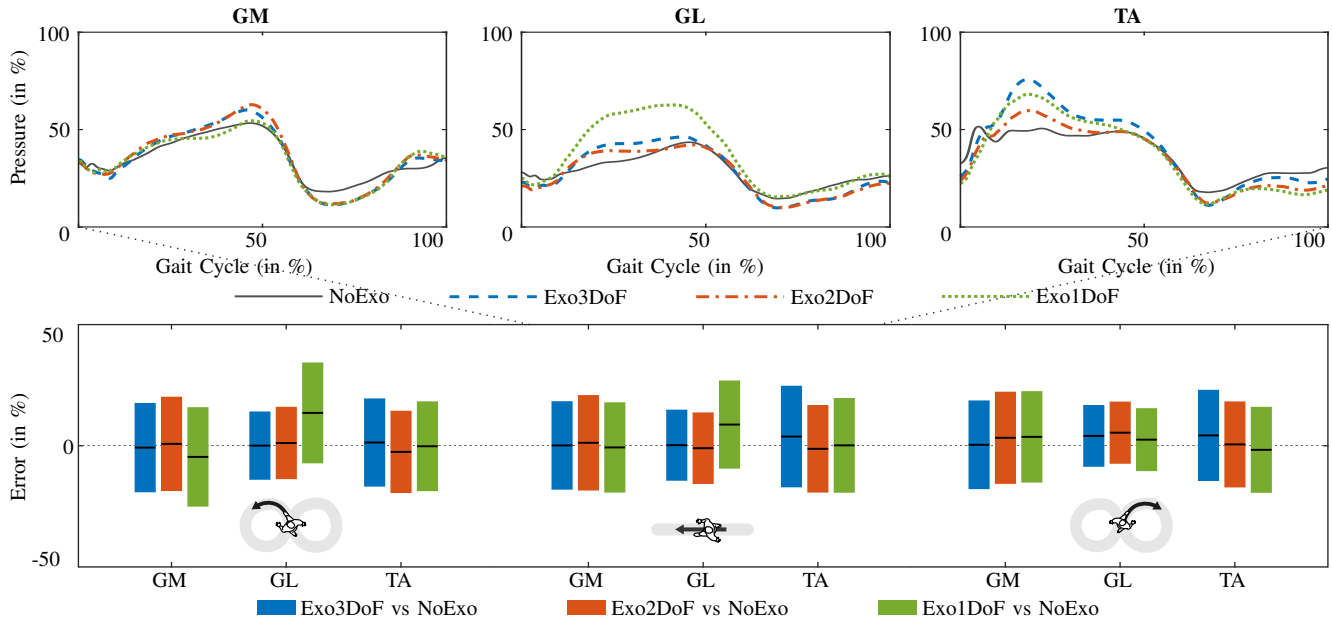

Fig. 6: Comparison of the FMG signals of each configuration per muscle: the normalized mean pressure measured in a full gait cycle during walking straight in each muscle separately (**top**), the FMG signal error with its mean (solid black line) and standard deviation (colored bar) as the difference between each exoskeleton configuration and the *NoExo* configuration for each muscle and direction separately (**bottom**).

Assuming that the stance phase refers to about 60 % at the beginning of the gait cycle and the swing phase about 40 % towards the end during straight walking, the three muscles in all four configurations are more active during the stance phase and visibly reduce their activity just before or after the toe off and regain some of their activity along the swing phase.

During straight walking, the timing of GM and GL peak pressure does not visibly differ, reaching their peak towards the end of the stance phase at about 45 % of the gait cycle. However, the GL shows a wider, less pronounced peak amplitude. Although the peak of the mean TA signal is not distinguishable in the *NoExo* configuration, in all three exoskeleton configurations, it is most prominent at about 18 % of the gait cycle. Across all four configurations, the FMG signal of straight walking appears to represent the average of the signal of the two walking directions of the curve in both muscles, GM and GL.

The FMG activity increased (*NoExo, Exo1DoF*) or remained unchanged (*Exo3DoF, Exo2DoF*) for GM in the inner leg (right curve) compared to walking straight. In the outer leg (left curve), the FMG activity remained similar in all configurations except the *Exo1DoF* configuration where it decreased compared to walking straight. Additionally, in the latter configuration, the mean signal shows two peaks at 20 % and at 46 % of the gait cycle.

The GL muscle shows the maximum changes in FMG activity during curve walking. The peak amplitude of the mean FMG signals at about 46 % of the gait cycle maintained a similar amplitude in the outer leg (left curve) in all configurations except the *Exo1DoF* configuration, where it increased significantly compared to walking straight. The FMG activity of the inner leg (right curve) remains almost unchanged in the three exoskeleton configurations (*Exo3DoF, Exo2DoF, Exo1DoF*), but its magnitude is smaller in the *NoExo* configuration.

The TA muscle shows only moderate changes compared to the ankle extensor muscles, GM and GL. In all three exoskeleton configurations (*Exo3DoF, Exo2DoF, Exo1DoF*) the signals in all three directions exhibit a slightly more pronounced peak at about 18 % of the gait cycle, while in the *NoExo* configuration the activity is almost constant throughout the stance phase without showing a distinctive peak.

TABLE II: Peak Occurrence

		NoExo	**Exo3DoF**	**Exo2DoF**	**Exo1DoF**
GM	S	43.3 ± 19.3	38.6 ± 15.1	42.9 ± 16.1	41.3 ± 21.6
	L	46.1 ± 16.4	42.7 ± 14.5	47.9 ± 17.5	43.8 ± 26.9
	R	41.1 ± 11.0	40.0 ± 11.6	43.2 ± 13.2	42.4 ± 12.9
GL	S	38.2 ± 16.5	35.0 ± 15.1	39.0 ± 17.4	34.4 ± 13.5
	L	44.2 ± 8.1	41.1 ± 11.2	38.8 ± 13.2	39.8 ± 8.3
	R	31.3 ± 13.8	29.5 ± 12.4	26.8 ± 14.1	33.1 ± 20.7
TA	S	26.3 ± 20.1	28.7 ± 16.2	32.7 ± 15.3	25.1 ± 13.5
	L	27.4 ± 19.3	24.9 ± 16.7	31.3 ± 15.2	22.2 ± 12.7
	R	27.5 ± 19.9	24.1 ± 14.2	19.8 ± 9.4	19.1 ± 10.5

Values represent the mean and standard deviation in percent of the gait cycle.
S - *walk straight*, L - *walk left*, R - *walk right*

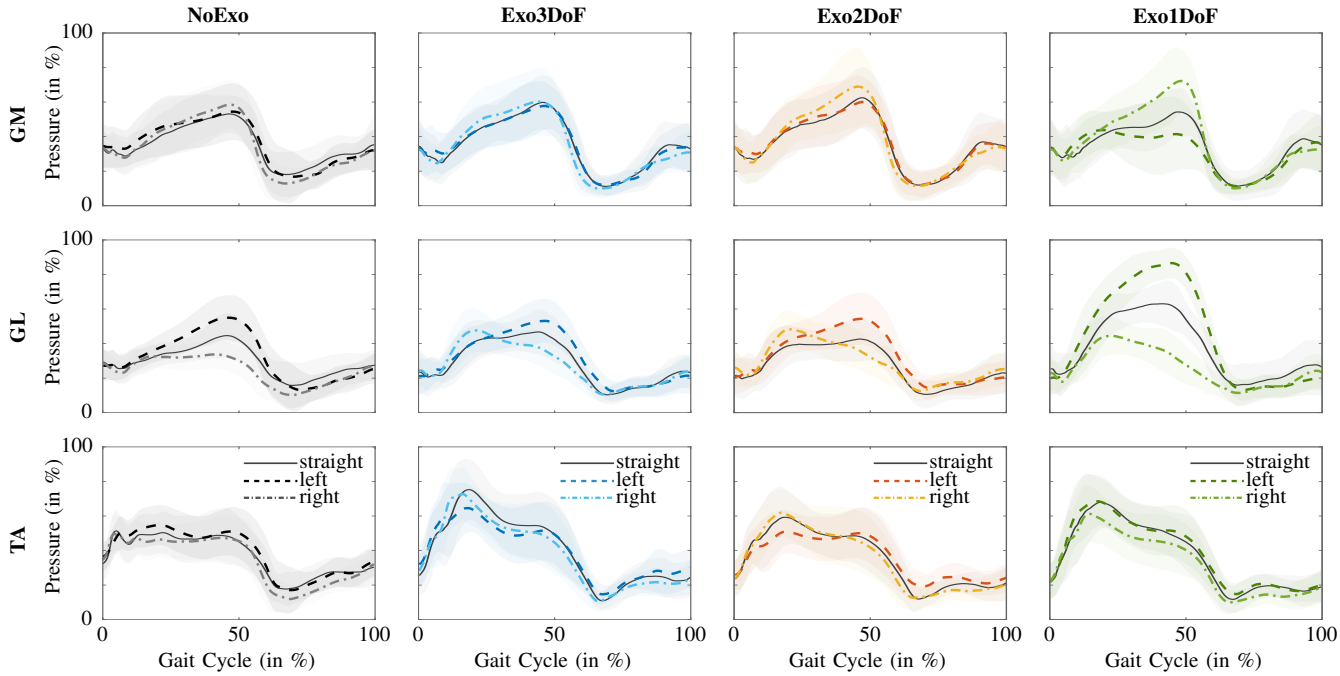

Fig. 7: Activity of the GM, GL and TA muscles during straight and curve walking. The figure shows the mean of the FMG signal amplitudes and their standard deviation computed from all samples over all participants in the three directions, *walk straight*, *walk left* and *walk right*. The plots are given over the gait cycle for each configuration (*NoExo*, *Exo3DoF*, *Exo2DoF*, *Exo1DoF*) separately.

Table II shows the calculated occurrence (as a percentage of the gait cycle) of the peak FMG (muscle activity) amplitude. The most significant variability between different walking directions across all configurations is observed in the GL muscle. During right curve walking, the peak FMG muscle activity is, on average, reached between 6.7 % to 12.9 % earlier than during left curve walking. This difference is most pronounced in the *NoExo* configuration, whereas the shift is almost halved in the *Exo1DoF* configuration. Although this effect is reduced in the GM muscle, the shift in the *Exo1DoF* configuration is also noticeably decreased. The TA muscle shows less noticeable variability between walking directions, but the shift in peak amplitude between left and right curve walking is also apparent in the *Exo2DoF* configuration. In all configurations, the GL displays earlier muscle activity than the GM muscle.

VI. Discussion

This user study investigates how decreasing the number of DoF in an ankle exoskeleton mechanism affects the FMG signal in the muscles of the lower limb during straight and curve walking. We analyze the variations in different configurations within a single task and compare the impact of curve walking on the results with that of walking straight, where the additional RoM of turning is expected to have a more notable effect.

Comparison of the three exoskeleton configurations with the *NoExo* configuration revealed that the *Exo1DoF* configurations showed the highest error from the FMG signal recorded without the exoskeleton, similar to the previous findings in EMG [26]. The findings align with the kinesiology of walking, highlighting the IN/EV's greater significance compared to the IR/ER during walking [29]. Moreover, the *Exo1DoF* configuration exhibits the most substantial misalignment, potentially impacting the quality of the FMG signal due to shear forces. Additionally, there is a visible difference between left and right walking with the error being higher for walking a right curve. This might result from the exoskeleton being on the right leg and thus on the inner leg while walking right. The reduced radius of the curvature leads to the need of a more pronounced turn on the loaded inner leg and therefore the need of IN/EV and IR/ER. However, the *Exo2DoF* configuration exhibits a degree of deviation that is not visibly greater than that of the *Exo3DoF* configuration. Both demonstrate high similarity across all configurations and locomotive directions. The TA muscle even manifest a reduced degree of deviation in the *Exo2DoF* configuration across all locomotive directions. These phenomena could potentially be attributed to the movement of soft tissues; the restriction of the IR/ER in the *Exo2DoF* configuration does not fully negate the inherent motion, as the movement of the soft tissue located beneath the cuff axial to the shank itself is not eliminated but increases with reduced DoF [28].

While the FMG signal of the GM exhibits a more pronounced peak, the trajectory of the GM signal shows a wider peak with each reduction of the DoF in the exoskeleton. However, the spatial errors of signal characteristics, such as

maximum and minimum positions, remain relatively consistent across the configurations. The TA demonstrates its most substantial variability as a result of the exoskeleton's attachment. In the *NoExo* configuration, the muscle maintains a comparable mean activity level during the stance phase in all locomotion directions, with only slight variations. However, with the exoskeleton mounted, it exhibits a notable peak following the foot's loading response, only to return to the amplitude observed during the stance phase without the exoskeleton. This phenomenon could potentially be attributed to the weight of the exoskeleton and the rigidity of the foot frame. These factors might decrease the required muscle strength during the heel strike phase due to gravitational forces, but conversely, they could enhance it during the rolling of the foot. However, an expected increase due to the weight during the initial and terminal swing phase, and thus reinforced dorsiflexion compared to the ankle extensor muscles, did not occur. The only effect observed is the amplitude decreased in the swing phase with each DoF reduction.

Although the FMG signal visibly differs from that of EMG in terms of its trajectory and characteristics, the results demonstrate similarities with previous studies focused on straight and curved walking without an exoskeleton [23], [24]. Specifically, the FMG signal exhibited the most notable changes in the GM and GL, which showed very prominent, opposite temporal changes during right curve motion, with the outer leg muscle being contracted before the inner leg muscle. This finding is consistent with previous research [23], which indicated that the degree of curvature affects the degree of temporal changes. During the right curve motion, the participant followed a tighter curve with the relevant leg, resulting in a shorter stride length for the inner leg compared to the outer leg. Additionally, previous research indicates that the duration of the stance phase was reduced, which could explain the temporal shift of maximum muscle activity in the inner leg muscle during walking on the right curve. However, only limited temporal changes were observed between the two muscles during the motion of the left curve, but the reported change consistently indicates earlier activity in the posterolateral than the posteromedial muscle. In addition, these findings are consistent with the musculoskeletal motion of the subtalar joint during walking. The subtalar joint is rapidly everted after heel strike and reverses its direction towards inversion before regaining a neutral position at the end of the stance phase [29]. With a reduced number of DoF, the effect is decreased, especially in the *Exo1DoF* configuration, where the IN/EV is completely restricted.

Our user study, while providing valuable insights, is not without its limitations. The evaluation was conducted with an exoskeleton on only one leg, leading to a disparity in weight distribution between the two legs. The weight of the un-powered exoskeleton is a significant factor that should not be overlooked, as it could have an impact on the user's experience and the study's outcomes. Furthermore, the current study did not account for shear forces, which may influence the results in restricted configurations. The investigation of shear forces was beyond the scope of the study; however, in [28], the rotation of the cuff was reported based on motion capture data which indicates a possible presence of such forces.

The current cuff design did not fully accommodate for different calf shapes of all participants. This resulted in data outliers when compared to participants with a better fit. The large inter-subject and inter-direction variations indicate the complexity of the task and the individual differences among participants. The absence of isometric measurements to determine maximum muscle pressure is a notable limitation. Instead, the minimum and maximum of the measured data were used for normalization, which may not accurately reflect the actual muscle pressure.

Another limitation was the absence of a specific walking speed. This could have led to a reduction in walking speed during curve walking or in the different configurations, potentially resulting in increased or decreased muscular activity. In addition, the study did not achieve steady-state walking as the distances were too short. This could potentially affect the reliability of our findings.

Future studies should aim to address these limitations to provide a deeper understanding of the performance of the exoskeleton and the effects of ankle motion restriction on the user.

VII. Conclusion

This paper studies the effect of reducing the number of DoF in an un-powered ankle exoskeleton mechanism on the FMG signal in the muscles of the lower limb during both straight and curved walking.

We analyzed variations in different configurations within a single walking direction and the impact of curve walking on the FMG signal. The findings reveal notable changes when both IN/EV and IR/ER were restricted compared to walking without an exoskeleton. However, solely locking IR/ER did not yield an evident effect across all locomotion directions. Our results indicate that ankle exoskeletons featuring two to three DoF produce more natural FMG muscle activity patterns. Hence, it is crucial to account for the number of DoF when designing FMG-based exoskeleton control systems.

Analysis of variations between straight and curve walking revealed observable changes in FMG depending on the legs and curves, which are related to modifications reported in the temporal and spatial gait parameters. The findings indicate that variations in walking direction can be identified using FMG and therefore utilized to modify the exoskeleton's control for each leg accordingly.

Future research will focus on more quantitative statistical evaluations that consider both legs simultaneously with integrated sensor units that measure normal and shear forces to increase the validity of the findings. Studies will incorporate consistent, steady-state motion in all locomotion directions and be validated on a larger scale study with additional activities of daily living.

ACKNOWLEDGMENT

The authors would like to thank the students Adnan Üğür and Jonathan Stockhorst for their support in conducting the user pilot study and post-processing the data and Tobias Möller (Institute of Sports and Sports Science, KIT) for reviewing the manuscript.

REFERENCES

[1] K. A. Shorter, J. Xia, E. T. Hsiao-Wecksler, W. K. Durfee, and G. F. Kogler, "Technologies for Powered Ankle-Foot Orthotic Systems: Possibilities and Challenges," *IEEE/ASME Transactions on Mechatronics*, vol. 18, no. 1, pp. 337–347, 2013.

[2] M. Dežman, C. Marquardt, and T. Asfour, "Ankle exoskeleton with a symmetric 3 dof structure for plantarflexion assistance," in *IEEE International Conference on Robotics and Automation (ICRA)*, Yokohama, Japan, May 2024.

[3] K. L. Poggensee and S. H. Collins, "How Adaptation, Training, and Customization Contribute to Benefits from Exoskeleton Assistance," *Science Robotics*, vol. 6, no. 58, p. eabf1078, Sep. 2021.

[4] M. Vlutters, E. Van Asseldonk, and H. Van Der Kooij, "Reduced center of pressure modulation elicits foot placement adjustments, but no additional trunk motion during anteroposterior-perturbed walking," *Journal of Biomechanics*, vol. 68, pp. 93–98, Feb. 2018.

[5] J. D. Hsu, J. W. Michael, J. R. Fisk, and American Academy of Orthopaedic Surgeons, Eds., *AAOS Atlas of Orthoses and Assistive Devices*, 4th ed. Philadelphia: Mosby/Elsevier, 2008.

[6] R. C. Browning, J. R. Modica, R. Kram, and A. Goswami, "The effects of adding mass to the legs on the energetics and biomechanics of walking," *Medicine & Science in Sports & Exercise*, vol. 39, no. 3, pp. 515–525, 2007, publisher: LWW.

[7] Z. S. Mahdian, H. Wang, M. I. M. Refai, G. Durandau, M. Sartori, and M. K. MacLean, "Tapping Into Skeletal Muscle Biomechanics for Design and Control of Lower Limb Exoskeletons: A Narrative Review," *Journal of Applied Biomechanics*, vol. 39, no. 5, pp. 318 – 333, 2023, place: Champaign IL, USA Publisher: Human Kinetics.

[8] J. Wang, D. Wu, Y. Gao, X. Wang, X. Li, G. Xu, and W. Dong, "Integral Real-time Locomotion Mode Recognition Based on GA-CNN for Lower Limb Exoskeleton," *Journal of Bionic Engineering*, Jul. 2022.

[9] C. D. Joshi, U. Lahiri, and N. V. Thakor, "Classification of gait phases from lower limb EMG: Application to exoskeleton orthosis," in *2013 IEEE Point-of-Care Healthcare Technologies (PHT)*, Jan. 2013, pp. 228–231, iSSN: 2377-5270.

[10] J. Taborri, E. Palermo, S. Rossi, and P. Cappa, "Gait Partitioning Methods: A Systematic Review," *Sensors*, vol. 16, no. 1, 2016.

[11] S. Jiang, P. Kang, X. Song, B. Lo, and P. B. Shull, "Emerging Wearable Interfaces and Algorithms for Hand Gesture Recognition: A Survey," *IEEE Reviews in Biomedical Engineering*, pp. 1–1, 2021.

[12] M. R. U. Islam and S. Bai, "Effective Multi-Mode Grasping Assistance Control of a Soft Hand Exoskeleton Using Force Myography," *Frontiers in Robotics and AI*, vol. 7, p. 139, 2020.

[13] Z. G. Xiao and C. Menon, "Performance of forearm FMG and sEMG for estimating elbow, forearm and wrist positions," *Journal of Bionic Engineering*, vol. 14, no. 2, pp. 284–295, 2017.

[14] X. Jiang, L.-K. Merhi, Z. G. Xiao, and C. Menon, "Exploration of Force Myography and surface Electromyography in hand gesture classification," *Medical Engineering & Physics*, vol. 41, pp. 63–73, Mar. 2017.

[15] M. R. Islam and S. Bai, "A novel approach of FMG sensors distribution leading to subject independent approach for effective and efficient detection of forearm dynamic movements," *Biomedical Engineering Advances*, vol. 4, p. 100062, 2022.

[16] X. Jiang, H. T. Chu, Z. G. Xiao, L.-K. Merhi, and C. Menon, "Ankle positions classification using force myography: An exploratory investigation," in *2016 IEEE Healthcare Innovation Point-Of-Care Technologies Conference (HI-POCT)*, Nov. 2016, pp. 29–32.

[17] X. Jiang, L. Tory, M. Khoshnam, K. Chu, and C. Menon, "Exploration of Gait Parameters Affecting the Accuracy of Force Myography-Based Gait Phase Detection*," in *2018 7th IEEE International Conference on Biomedical Robotics and Biomechatronics (Biorob)*, Aug. 2018, pp. 1205–1210, iSSN: 2155-1782.

[18] X. Jiang, K. H. Chu, and C. Menon, "An easy-to-use wearable step counting device for slow walking using ankle force myography," in *2017 IEEE International Conference on Systems, Man, and Cybernetics (SMC)*, 2017, pp. 2219–2224.

[19] M. R. U. Islam, K. Xu, and S. Bai, "Position Sensing and Control with FMG Sensors for Exoskeleton Physical Assistance," in *Wearable Robotics: Challenges and Trends*, ser. Biosystems & Biorobotics, M. C. Carrozza, S. Micera, and J. L. Pons, Eds. Cham: Springer International Publishing, 2019, pp. 3–7.

[20] X. Zhou, C. Wang, L. Zhang, J. Liu, G. Liang, and X. Wu, "Continuous Estimation of Lower Limb Joint Angles From Multi-Stream Signals Based on Knowledge Tracing," *IEEE Robotics and Automation Letters*, vol. 8, no. 2, pp. 951–957, Feb. 2023.

[21] C. Marquardt, P. Weiner, M. Dežman, and T. Asfour, "Embedded barometric pressure sensor unit for force myography in exoskeletons," in *IEEE/RAS International Conference on Humanoid Robots (Humanoids)*, Ginowan, Okinawa, Japan, 2022, pp. 67–73.

[22] G. Courtine and M. Schieppati, "Human walking along a curved path. II. Gait features and EMG patterns," *European Journal of Neuroscience*, vol. 18, no. 1, pp. 191–205, 2003.

[23] G. Courtine, C. Papaxanthis, and M. Schieppati, "Coordinated modulation of locomotor muscle synergies constructs straight-ahead and curvilinear walking in humans," *Experimental Brain Research*, vol. 170, no. 3, pp. 320–335, Apr. 2006.

[24] K. Duval, K. Luttin, and T. Lam, "Neuromuscular strategies in the paretic leg during curved walking in individuals post-stroke," *Journal of Neurophysiology*, vol. 106, no. 1, pp. 280–290, Jul. 2011, publisher: American Physiological Society.

[25] R. Gross, F. Leboeuf, M. Lempereur, T. Michel, B. Perrouin-Verbe, S. Vieilledent, and O. Rémy-Néris, "Modulation of lower limb muscle activity induced by curved walking in typically developing children," *Gait & Posture*, vol. 50, pp. 34–41, Oct. 2016.

[26] R. Ranaweera, A. Weerasingha, W. Withanage, A. Pragnathilaka, R. Gopura, T. Jayawardana, and G. Mann, "Effects of Restricting Ankle Joint Motions on Muscle Activity: Preliminary Investigation with an Unpowered Exoskeleton," in *2022 Moratuwa Engineering Research Conference (MERCon)*, Jul. 2022, pp. 1–6, iSSN: 2691-364X.

[27] N. Aliman, R. Ramli, and S. M. Haris, "Design and development of lower limb exoskeletons: A survey," *Robotics and Autonomous Systems*, vol. 95, pp. 102–116, 2017, publisher: Elsevier.

[28] M. Dežman, C. Marquardt, A. Üğür, and T. Asfour, "Influence of motion restrictions in an ankle exoskeleton on gait kinematics and stability in straight walking," in *IEEE/RAS/EMBS International Conference on Biomedical Robotics and Biomechatronics (BioRob)*, 2024, [accepted to IEEE Transactions on Medical Robotics & Bionics].

[29] D. A. Neumann and E. E. Rowan, *Kinesiology of the musculoskeletal system: foundations for physical rehabilitation*. Mosby, Mar. 2002.